scientific reports

Check for updates

OPEN

Enhanced effect of the immunosuppressive soluble HLA-G2 homodimer by site-specific PEGylation

Chisato Yamada[1,7], Kimiko Kuroki[1,7]✉, Naoyoshi Maeda[2,3], Hiroshi Watanabe[1], Ami Takahashi[1] & Katsumi Maenaka[1,2,4,5,6]✉

Human leukocyte antigen (HLA)-G is a nonclassical HLA class I molecule that has an immunosuppressive effect mediated by binding to immune inhibitory leukocyte immunoglobulin-like receptors (LILR) B1 and LILRB2. A conventional HLA-G isoform, HLA-G1, forms a heterotrimeric complex composed of a heavy chain (α1-α3 domains), β2-microglobulin (β2m) and a cognate peptide. One of the other isoforms, HLA-G2, lacks a α2 domain or β2m to form a nondisulfide-linked homodimer, and its ectodomain specifically binds to LILRB2 expressed in human monocytes, macrophages, and dendritic cells. The administration of the ectodomain of HLA-G2, designated the soluble HLA-G2 homodimer, showed significant immunosuppressive effects in mouse models of rheumatoid arthritis and systemic lupus erythematosus, presumably by binding to a mouse ortholog of LILRB2, paired immunoglobulin-like receptor B. However, the refolded soluble HLA-G2 homodimer used in these studies tends to aggregate and degrade; thus, its stability for clinical use has been a concern. In the present study, we improved the stability of the refolded soluble HLA-G2 homodimer via a site-directed PEGylation method. PEGylation at an original free cysteine residue, Cys42, resulted in increased lyophilization and thermal and serum stability. Furthermore, the PEGylated soluble HLA-G2 homodimer could better suppress atopic symptoms in mice than the non-PEGylated homodimer. These results suggest that PEGylated soluble HLA-G2 homodimers could be candidates for immunosuppressive biologics that specifically target LILRB2-positive myelomonocytic antigen-presenting cells.

Keywords HLA-G2, LILR, PEGylation, Immune checkpoint, Immunosuppressive

Human leukocyte antigen (HLA)-G is a nonclassical major histocompatibility complex (MHC) class I molecule. HLA-G is involved in escape from maternal immune responses during pregnancy. HLA-G has four functional splicing isoforms (HLA-G1 and HLA-G2; membrane-bound forms, HLA-G5 and HLA-G6; soluble forms). Because the composition of N-terminal functional domains is identical, hereafter, HLA-G1 and HLA-G5 are simply called HLA-G1, and HLA-G2 and HLA-G6 are called HLA-G2 in this paper. HLA-G1, a typical structure composed of a heavy chain (α1, α2 and α3 domains), a peptide and β2-microglobulin (β2m), can exist as β2m-free forms and homodimers (Supplementary Fig. 1)[1–3]. The characteristics of the HLA-G1 isoform have been elucidated to suppress the proliferation of $CD4^+$ T cells or the cytotoxic activity of $CD8^+$ T cells and natural killer (NK) cells[4–6]. These functions of HLA-G1 are transmitted through immune inhibitory receptors, leukocyte immunoglobulin-like receptor B1 (LILRB1) and LILRB2. We previously reported that soluble HLA-G1 could also bind to paired immunoglobulin-like receptor (PIR)-B, a mouse homolog of LILRB2, and showed significant anti-inflammatory effects in collagen-induced arthritis (CIA) and atopic dermatitis model mice[7,8]. Interestingly,

[1]Laboratory of Biomolecular Science, Faculty of Pharmaceutical Sciences, Hokkaido University, Sapporo 060-0812, Japan. [2]Center for Research and Education On Drug Discovery, Faculty of Pharmaceutical Sciences, Hokkaido University, Sapporo 060-0812, Japan. [3]School of Pharmaceutical Sciences, Health Sciences University of Hokkaido, Hokkaido 061-0293, Japan. [4]Institute for Vaccine Research and Development (HU-IVReD), Hokkaido University, Sapporo 001-0021, Japan. [5]Global Station for Biosurfaces and Drug Discovery, Hokkaido University, Sapporo 060-0812, Japan. [6]Faculty of Pharmaceutical Sciences, Kyushu University, Fukuoka 812-8582, Japan. [7]Chisato Yamada and Kimiko Kuroki have contributed equally. ✉email: k-kimiko@pharm.hokudai.ac.jp; maenaka@pharm.hokudai.ac.jp

soluble disulfide-bonded HLA-G1 homodimers via Cys42 exert more significant effects than soluble HLA-G1 monomers do[7]. Therefore, an avidity effect on receptor binding by dimerization of HLA-G1 might be important for enhancing tolerance.

Another physiologically functional HLA-G isoform, HLA-G2, lacks the α2 domain and exhibits a nondisulfide-linked homodimer despite having Cys42 (Supplementary Fig. 1). We previously reported that soluble HLA-G2 homodimers specifically bind to immobilized LILRB2 but not to LILRB1[3]. Moreover, the binding of soluble HLA-G2 homodimers to LILRB2 is much stronger (apparent $K_d \sim 1.7$ nM)[3] than that of soluble HLA-G1 homodimers (apparent $K_d \sim 750$ nM)[9]. In mice, the soluble HLA-G2 homodimer has been shown to have an immunosuppressive effect on CIA mice with lower-dose administration than the soluble HLA-G1 homodimer[7,10]. With respect to receptor distribution, the expression of LILRB2 is restricted to myeloid antigen-presenting cells (APCs), such as monocytes, macrophages, and dendritic cells (DCs), whereas LILRB1 is additionally expressed on lymphoid cells, including B cells and subsets of NK and T cells. Mouse PIR-B is expressed in myeloid APCs and B cells, similar to LILRB2. These observations suggest that soluble HLA-G2 homodimer-LILRB2 signaling is sufficient to suppress pathological inflammation or autoimmune responses in humans. However, the refolded soluble recombinant HLA-G2 homodimeric protein expressed in *Escherichia coli* tends to aggregate or degrade during storage.

In this study, to improve the stability of the soluble HLA-G2 homodimer, a covalent attachment of polyethylene glycol (PEG) was used. As a result of screening the position and molecular weight of PEG in PEGylation, the soluble HLA-G2 homodimer modified with 20 kDa PEG at the Cys42 residue (PEG20K-HLA-G2) was suggested to be a promising candidate in terms of purity and receptor-binding activity. PEG20K-HLA-G2 showed increased biophysical stability against lyophilization, heat, and fetal bovine serum (FBS). In addition, PEG20K-HLA-G2 had greater therapeutic effects than non-PEGylated soluble HLA-G2 homodimer (sHLA-G2) in atopic dermatitis model mice. These findings demonstrated that PEGylation with 20 kDa PEG at Cys42 of a soluble HLA-G2 homodimer (PEG20K-HLA-G2) is a practical approach for enhancing the immunosuppressive effects in clinical use.

Materials and methods

PEG reagent

Pharmaceutical-grade PEG reagents that possess NHS (N-hydroxysuccinimide)-active esters (SUNBRIGHT ME-400CS; Mw 43,231 Da, NOF Cooperation) or maleimide groups (SUNBRIGHT ME-400MA; 42,653 Da, ME-200MAOB; 20,841 Da, ME-100MA; 10,303 Da, ME-050 M; 5,393 Da, NOF Cooperation) were used for the PEGylation of soluble recombinant HLA-G2 homodimers.

Preparation of soluble HLA-G2 homodimers and recombinant LILRB2 proteins

HLA-G2 (Gly1-Trp182) and the two N-terminal domains (D1D2) of LILRB2 (Gly1-Leu197) with a C-terminal biotinylation tag (ASLHHILDAQKMVWNHR) were expressed in *Escherichia coli*, refolded via the dilution method, and the refolded disulfide-bond-free soluble HLA-G2 homodimer (Supplementary Fig. 1) was purified as previously described[3,10,11]. Briefly, soluble HLA-G2 homodimers and LILRB2 were expressed in BL21(DE3) pLysS competent cells (Novagen) for in vitro analyses or in ClearColi BL21(DE3) competent cells (Lucigen) for in vivo analysis. All the refolded proteins were purified by size exclusion chromatography (SEC) via a HiLoad 26/60 Superdex75 pg column (GE Healthcare) equilibrated with SEC buffer (20 mM Tris–HCl, pH 8.0, 100 mM NaCl).

To consider the PEGylation site using PEG-maleimide reagents, single cysteine residue-introduced mutants were constructed from the HLA-G2 C42S mutant plasmid[3]. HLA-G2 N86C has a cysteine residue at the glycosylation site, asparagine 86 of HLA-G2 C42S, and HLA-G2 CG has a cysteine residue at the C-terminal membrane proximal region of HLA-G2 C42S. These HLA-G2 mutants were prepared in the same way as the soluble HLA-G2 homodimer. LILRB2 was biotinylated with the BirA enzyme for one hour at 30 °C. The biotinylated LILRB2 was finally purified by SEC using a Superdex75 10/300 GL column (GE Healthcare).

PEGylation of soluble HLA-G2 homodimers

The purified soluble HLA-G2 homodimer was concentrated, and the buffer was exchanged with PEGylation buffer (PBS, 5 mM EDTA) via Amicon Ultra (Millipore). The soluble HLA-G2 homodimer was incubated with ten molar equivalents of 40 kDa PEG reagent at 25 °C for 2 h for random PEGylation at lysine residues. For site-specific PEGylation in a cysteine residue, after vacuum degassing for one hour on ice to prevent oxidation, the soluble HLA-G2 homodimer was incubated with 0.1 mM tris(2-carboxyethyl)phosphine (TCEP) and ten molar equivalents of each PEG mixture at 4 °C overnight. The PEGylated soluble HLA-G2 homodimer was detected via SDS-PAGE following coomassie brilliant blue (CBB) staining and barium iodide (BaI_2) staining. BaI_2 specifically stains PEG molecules with very high sensitivity and thus can resolve PEG-attached HLA-G2, which is difficult to identify by CBB staining because all proteins are visible. BaI_2 staining was performed by shaking the SDS-PAGE gel in 5% BaI_2 solution (15 min), water (30 min), and 0.1 M iodide solution (5 min). PEGylated soluble HLA-G2 homodimers (PEG5K-HLA-G2, PEG10K-HLA-G2, PEG20K-HLA-G2, and PEG40K-HLA-G2) were purified via SEC using a Superdex200 10/300 GL column (GE Healthcare) with SEC buffer (20 mM Tris–HCl, pH 8.0, 100 mM NaCl).

Surface plasmon resonance (SPR) analysis

SPR analysis was performed via a BIAcore3000 instrument (GE Healthcare) at 25 °C. For the random PEGylated soluble HLA-G2 homodimer protein (randomPEG-HLA-G2), either the C-terminal biotinylated PIR-B or chemically biotinylated BSA (as a control) was immobilized on the surface of the sensor chip CM5 (GE Healthcare) covalently coupled with streptavidin. The purified recombinant soluble HLA-G2 homodimer protein

in HBS-EP running buffer (10 mM Hepes, 150 mM NaCl, 3 mM EDTA, 0.005% Tween-20, GE Healthcare) was injected over each flow cell as a positive control (sHLA-G2).

For the site-specific PEGylated soluble HLA-G2 homodimer proteins, biotinylated LILRB2 and chemically biotinylated BSA were immobilized on the sensor chip CAP via a Biotin CAPture Kit (GE Healthcare) (immobilization level: 500–700 RU). sHLA-G2 and each PEGylated soluble HLA-G2 homodimer protein were injected over the flow cells as analyte proteins. For kinetic analysis, sHLA-G2 or PEGylated soluble HLA-G2 homodimer proteins were twofold serially diluted with HBS-EP buffer (GE Healthcare). They were injected into each flow cell independently at 10 µL/min because the regeneration conditions of the sensor chip could not be determined. The apparent K_d value was calculated via local fitting via the 1:1 Langmuir binding model with BIAevaluation version 4.1.1 (GE Healthcare).

Thermal stability

The purified sHLA-G2 (control) and PEG20K-HLA-G2 were incubated at 50 and 60 °C for 7, 24, and 48 h, respectively. Thermal stability was evaluated by SDS-PAGE analysis under nonreducing conditions and CBB staining.

Serum stability

The purified sHLA-G2 (control) and PEG20K-HLA-G2 mixed with 10% FBS (Biosera, Lot No. 10777) at a volume ratio of 1:1 (v/v) were incubated at 37 °C for 22–30 h. The stability of the sHLA-G2 and PEG20K-HLA-G2 proteins was evaluated by western blotting. An anti-HLA-G antibody that can bind to the HLA-G2 isoform, MEM-G1 (Abcam)[12], and an anti-mouse-IgG (Fc)-horseradish peroxidase (HRP) (Thermo Fisher Scientific) were used as primary and secondary antibodies, respectively. An ImageQuant LAS4000 mini instrument (GE Healthcare) was used for detection.

Stability during lyophilization

The purified sHLA-G2 (control) and PEG20K-HLA-G2 in HBS-EP buffer were lyophilized and redissolved in an equivalent volume of Milli-Q water. Stability was evaluated by SDS-PAGE under nonreducing conditions and CBB staining. The receptor binding activity was examined via SPR analysis as described previously.

Immunosuppressive effect of PEGylated HLA-G2 in atopic model mice

Ten-week-old female NC/Nga mice were purchased from Japan SLC (Shizuoka, Japan) and maintained under specific pathogen-free conditions. The experiment was performed at the same time as the previous soluble HLA-G1 study and compared with the same data from the PBS and control groups (nontreated with *Dermatophagoides farinae* body (Dfb) ointment) (n = 4)[8]. The Dfb ointment (100 mg, Biostir, Inc.) was applied to the shaved skin and the surface of both ears. From the second induction, 4% SDS treatment to disrupt the mouse skin barrier was performed before Dfb ointment treatment, and the SDS/Dfb ointment treatments were repeated every three days for 15 days. Both ears were treated with 5 µg of purified recombinant sHLA-G2 (control) or PEG20K-HLA-G2 every other day for 20 days. Ear thickness was evaluated via dial thickness gauges (OZAKI MFG. Co., Ltd., Tokyo, Japan). Body weight changes were monitored twice a week. Pairwise multiple comparisons were analyzed via Tukey's test using EZR software, which is frequently used in biostatistics[13]. The significance level was set at $P < 0.05$.

All experiments were approved and performed in accordance with the guidelines of the Committee of Ethics on Animal Experiments at Hokkaido University.

Ethics approval

All experiments were approved and performed in accordance with the guidelines of the Committee of Ethics on Animal Experiments at Hokkaido University (No. 16-0063). The experiments were carried out in accordance with the ARRIVE guidelines.

Results

Random PEGylation of soluble HLA-G2 homodimers at lysine residues

To improve the stability of the soluble HLA-G2 homodimer (Supplementary Fig. 1), random PEGylation targeting lysine residues via 40 kDa PEG with NHS-active esters (ME-400CS) was performed. Compared with the negative control (BSA), sHLA-G2 (6.2 µM) showed a specific binding response (~ 100 RU) to its mouse receptor PIR-B (Fig. 1A). On the other hand, the same concentration of PEGylated soluble HLA-G2 homodimer (randomPEG-HLA-G2) lost the specific binding response to PIR-B (Fig. 1A). The refolded soluble HLA-G2 homodimer has four lysine residues (K68, K94, K151, and K183) in a monomer (Fig. 1B). Because all lysine residues can be spatially attached to PEG molecules (Fig. 1B), some of them are expected to be involved in binding to their receptors directly or indirectly.

Site-specific PEGylation of soluble HLA-G2 homodimers in a cysteine residue

To avoid steric hindrance of the receptor binding region on the soluble HLA-G2 homodimer, site-specific PEGylation was performed. A free cysteine residue located at the exposed surface of the EM structure of soluble HLA-G2 homodimers[3], Cys42, was targeted by a PEG-maleimide molecule (Fig. 2A HLA-G2, Fig. 2B). Four different sizes of PEG-maleimide molecules (5, 10, 20, and 40 kDa) were examined to determine the optimal molecular weight for the purification of the PEGylated soluble HLA-G2 homodimer by SEC. PEGylation of the soluble HLA-G2 homodimer was confirmed by SDS-PAGE and CBB or BaI_2 staining (Fig. 3A). The purity of the PEGylated soluble HLA-G2 homodimer after SEC depended on the PEG size. Although SDS-PAGE revealed that the PEG5K-attached soluble HLA-G2 homodimer (PEG5K-HLA-G2) could not be successfully purified

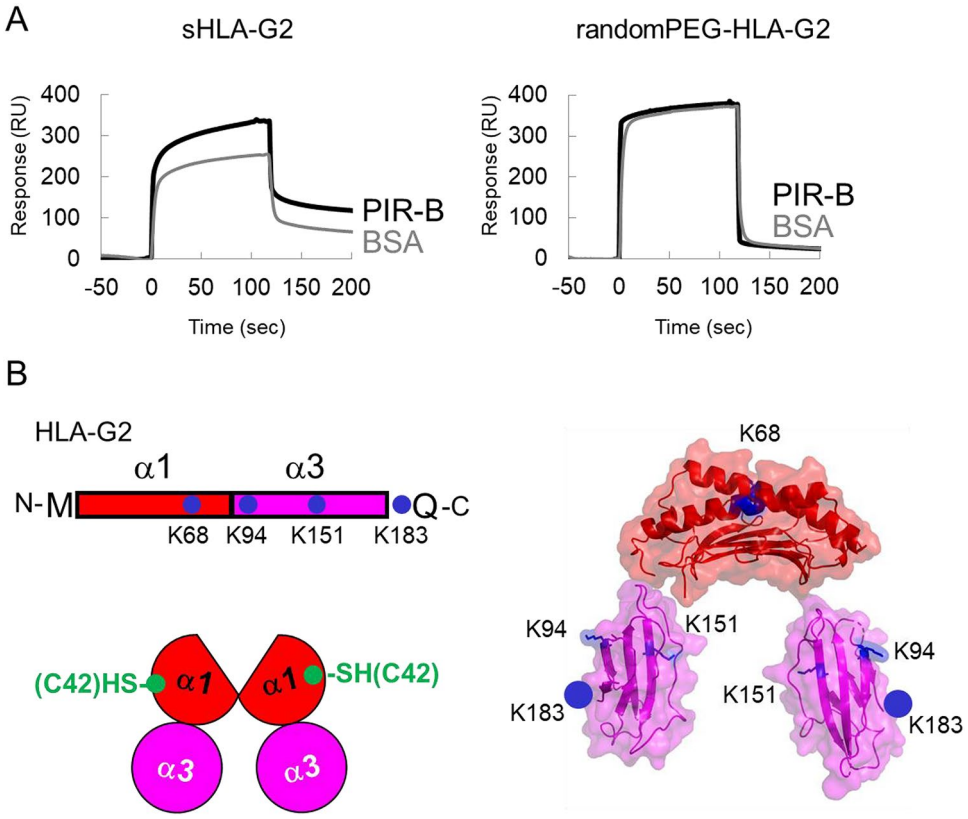

Fig. 1. Randomly PEGylated soluble HLA-G2 homodimer protein in lysine residues. (**A**) SPR analysis of HLA-G2 (6.2 μM, left) or PEGylated HLA-G2 in lysine residues (randomPEG-HLA-G2, 5.3 μM, right) to the immobilized PIR-B. Each soluble HLA-G2 homodimer protein was injected over the immobilized PIR-B (3000 RU, black line) and negative control BSA (2000 RU, gray line). The response of the SPR results to BSA was due to buffer mismatch and nonspecific interactions between the analytes and BSA. (**B**) Schematic diagram of the domain structure (left) and the model structure (right) of the soluble HLA-G2 homodimer[3]. The original Cys42 (green circle) and lysine residues (blue circle) are shown in the schematic structures (left). Three lysine residues are shown in the blue stick model (right). K183, which is not visible in the crystal structure of the soluble HLA-G1 monomer (PDB ID: 2DYP), is shown in the blue circle (right).

by SEC, the others seemed to be purified as a major band via SDS-PAGE (Fig. 3B). Among them, the yield of PEG20K-HLA-G2 was better than those of PEG10K and PEG40K (Fig. 3B), suggesting that PEG20K can be suitable for soluble HLA-G2 homodimer modification.

To determine the optimal position of PEG20K modification, soluble HLA-G2 homodimer mutants possessing a single free cysteine residue were constructed based on the C42S mutation of the soluble HLA-G2 homodimer to avoid undesirable PEG attachment (Fig. 2A). As candidate positions, Asn86 and the C-terminus were selected. (i) Asn86, which is responsible for a sugar modification (Asn86) of HLA-G, was substituted with cysteine (HLA-G2 N86C). (ii) Cysteine-glycine residues are attached at the C-terminal membrane-proximal site (HLA-G2 CG) (Fig. 2).

All soluble HLA-G2 homodimer proteins were successfully refolded and purified by SEC (Fig. 4A). Although all were successfully modified by PEG20K (Fig. 4A), the PEGylated soluble HLA-G2 N86C and HLA-G2 CG homodimers (PEG20K-HLA-G2 N86C and PEG20K-HLA-G2 CG, respectively) could not be purified well by SEC (Fig. 4B). Therefore, PEG20K-HLA-G2 was used for further in vitro and in vivo studies.

Binding activity of PEG20K-HLA-G2 to LILRB2

To examine the binding activity of PEG20K-HLA-G2 to its receptor LILRB2, SPR analysis was performed via a BIAcore3000 instrument. PEG20K-HLA-G2 and sHLA-G2 specifically bound to immobilized LILRB2 with a slow dissociation rate (Fig. 5A). The apparent K_d value of PEG20K-HLA-G2 to LILRB2 was comparable to that of sHLA-G2 (Fig. 5B). Thus, PEG20K-HLA-G2 is expected to have immunosuppressive functions as an anti-inflammatory biologic.

Stability of PEG20K-HLA-G2 in vitro

The stability of PEG20K-HLA-G2 and non-PEGylated sHLA-G2 (control) was examined against heat, serum, and lyophilization. The heat stability was evaluated by incubation at 50 °C or 60 °C for 7–48 h following SDS-PAGE under nonreducing conditions. During incubation, sHLA-G2 tended to oligomerize through disulfide

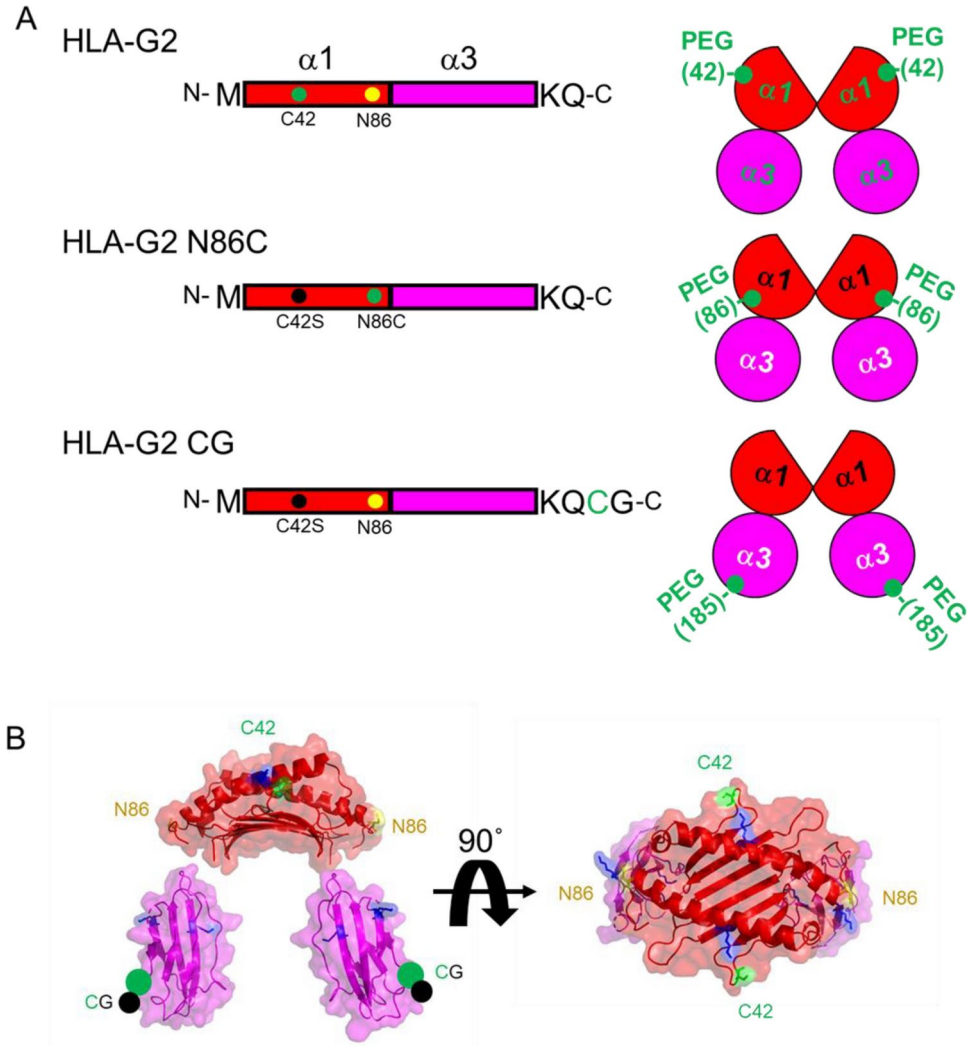

Fig. 2. The positions of the targeted residues on the soluble HLA-G2 homodimer for PEGylation. (**A**) Schematic diagram of the domain structures of soluble HLA-G2 homodimers and their mutants. The cysteine residues used for PEG attachment are shown in green circles (right). In HLA-G2 N86C and HLA-G2 CG, C42 was substituted for serine (C42S). (**B**) Model structure of soluble HLA-G2 homodimers[3]. The positions of the target residues for PEGylation are shown. All targeted residues are exposed on the surface of the soluble HLA-G2 homodimer. The lysine residues in the blue stick models targeted for random PEGylation (Fig. 1) are also shown.

bonds as a population with high molecular weights (mainly approximately 42 kDa) (Fig. 6A). Consistent with this finding, the 20 kDa band derived from sHLA-G2 disappeared in a time-dependent manner (Fig. 6A). On the other hand, PEG20K-HLA-G2 was stable at both temperatures (Fig. 6A). This result suggested that PEG20K-HLA-G2 can exist as homogenous molecules at high temperatures. Thus, the heat stability of the soluble HLA-G2 homodimer was improved by PEGylation.

To evaluate the stability of sHLA-G2 and PEG20K-HLA-G2 in serum, the purified HLA-G2 proteins were incubated with 5% FBS at 37 °C for 22–30 h. The band of sHLA-G2 disappeared faster than that of PEG20K-HLA-G2 (Fig. 6B).

Next, the stability and receptor binding activity after lyophilization were analyzed. Purified sHLA-G2 and PEG20K-HLA-G2 were lyophilized once and reconstituted in an equivalent volume of Milli-Q water. SDS-PAGE under nonreducing conditions revealed that both sHLA-G2 molecules were homogeneous without multimerization/aggregation via disulfide bonds or degradation products (Fig. 6C). SPR analysis revealed that the binding response of sHLA-G2 (0.6 μM) to LILRB2 was decreased after lyophilization compared with that of nonlyophilized HLA-G2, whereas the binding of PEG20K-HLA-G2 to LILRB2 did not change with lyophilization (Fig. 6D). In addition, each apparent K_D value was calculated to compare the binding affinity of PEG20K-HLA-G2 before and after lyophilization (Fig. 6E). Compared with the kinetic parameters of nonlyophilized sHLA-G2 proteins shown in Fig. 5B, the apparent K_D values of PEG20K-HLA-G2 and sHLA-G2 binding to LILRB2 were comparable after lyophilization (PEG20K-HLA-G2: 13.8×10^{-8} to 12.7×10^{-8} μM and sHLA-G2:

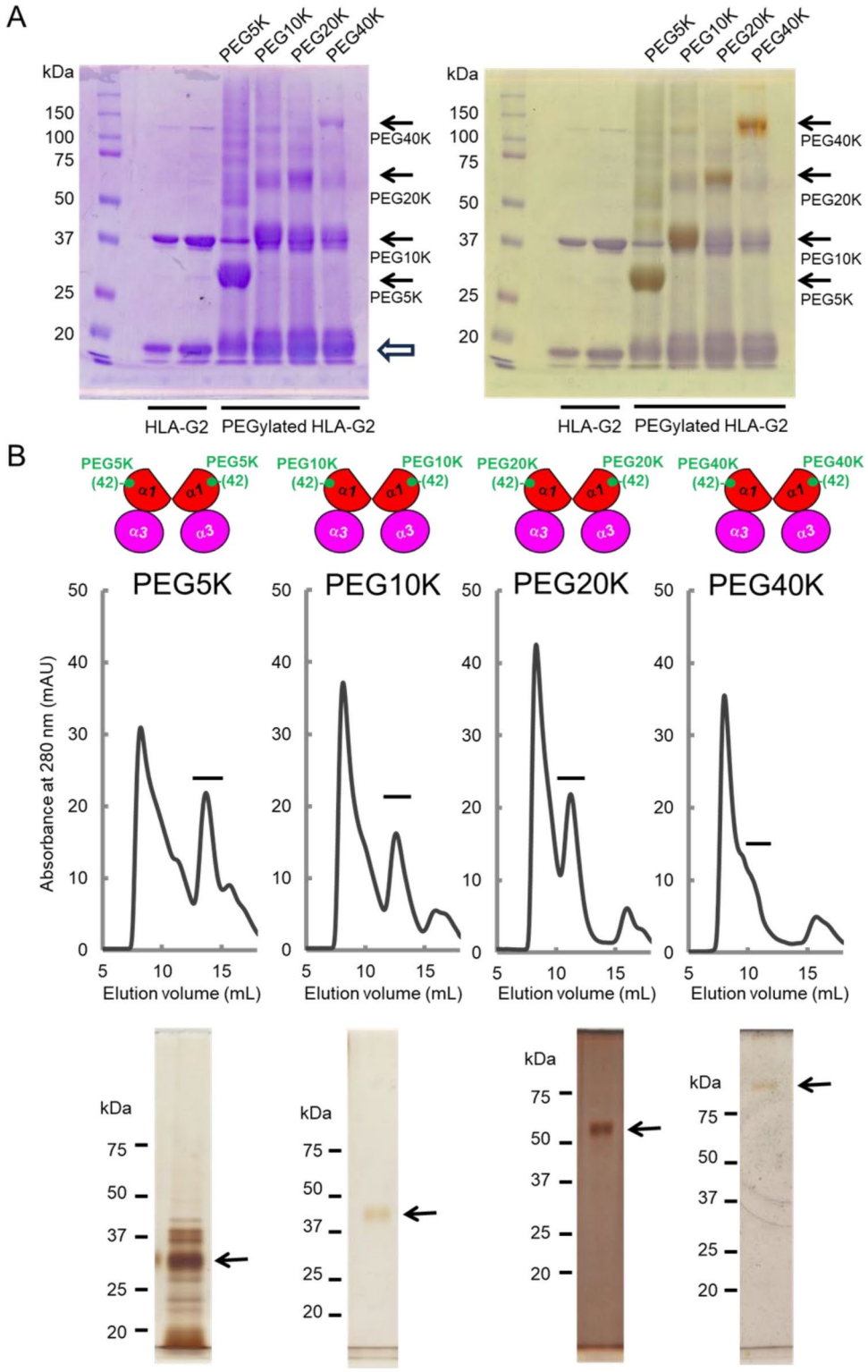

4.1×10^{-8} to 6.4×10^{-8} μM). This result indicated that reconstituted PEG20K-HLA-G2 and sHLA-G2 maintained their binding activity.

Evaluation of the anti-inflammatory effects of PEG20K-HLA-G2 in vivo

To evaluate the functional activity of PEG20K-HLA-G2 in vivo, the anti-inflammatory effects on the skin of atopic dermatitis model mice were examined. Similar to a previous soluble HLA-G1 study[8], the immunosuppressive effects of sHLA-G2 and PEG20K-HLA-G2 were also evaluated (Fig. 7A). Therefore, the clinical values of sHLA-G2 protein-administered mice were compared with those of the control groups shown in the soluble HLA-G1 study[8]. sHLA-G2 treatment did not cause overt toxicity, as shown by the change in body weight (Fig. 7B). Compared with PBS-treated mice, sHLA-G2- and PEG20K-HLA-G2-treated mice presented fewer symptoms at the macroscopic level, such as hemorrhage, scarring, and skin dryness (Fig. 7C). The ear thickness of the lesional

◂**Fig. 3**. PEGylation of soluble HLA-G2 homodimers by four different molecular weights of PEG-maleimide molecules. (**A**) SDS-PAGE analysis of the PEGylated soluble HLA-G2 homodimer mixture with each molecular size of PEG under nonreducing conditions followed by CBB (left) and BaI_2 (right) staining. The PEGylated proteins were detected as brown bands in BaI_2 staining. The non-PEGylated soluble HLA-G2 monomer separated in the SDS-PAGE gel (21 kDa) is indicated by a white arrow, and the black arrows indicate the PEGylated soluble HLA-G2 homodimer. Multimerization of the non-PEGylated soluble HLA-G2 homodimer resulted in the existence of a 42 kDa band due to disulfide bonding via Cys42. (**B**) Purification of the PEGylated soluble HLA-G2 homodimer proteins by SEC and SDS-PAGE analysis under nonreducing conditions followed by BaI_2 staining of the SEC fractions indicated by black lines in the chromatograms. The band derived from the PEGylated soluble HLA-G2 homodimer is indicated by black arrows. A schematic diagram of the domain structure of each soluble HLA-G2 homodimer is shown. A representative chromatogram of five (5 kDa) or six (10 kDa and 20 kDa) experiments is shown. The 40 kDa PEG experiment was performed once. See Supplementary Figs. 2 and 3 for the uncropped gel images.

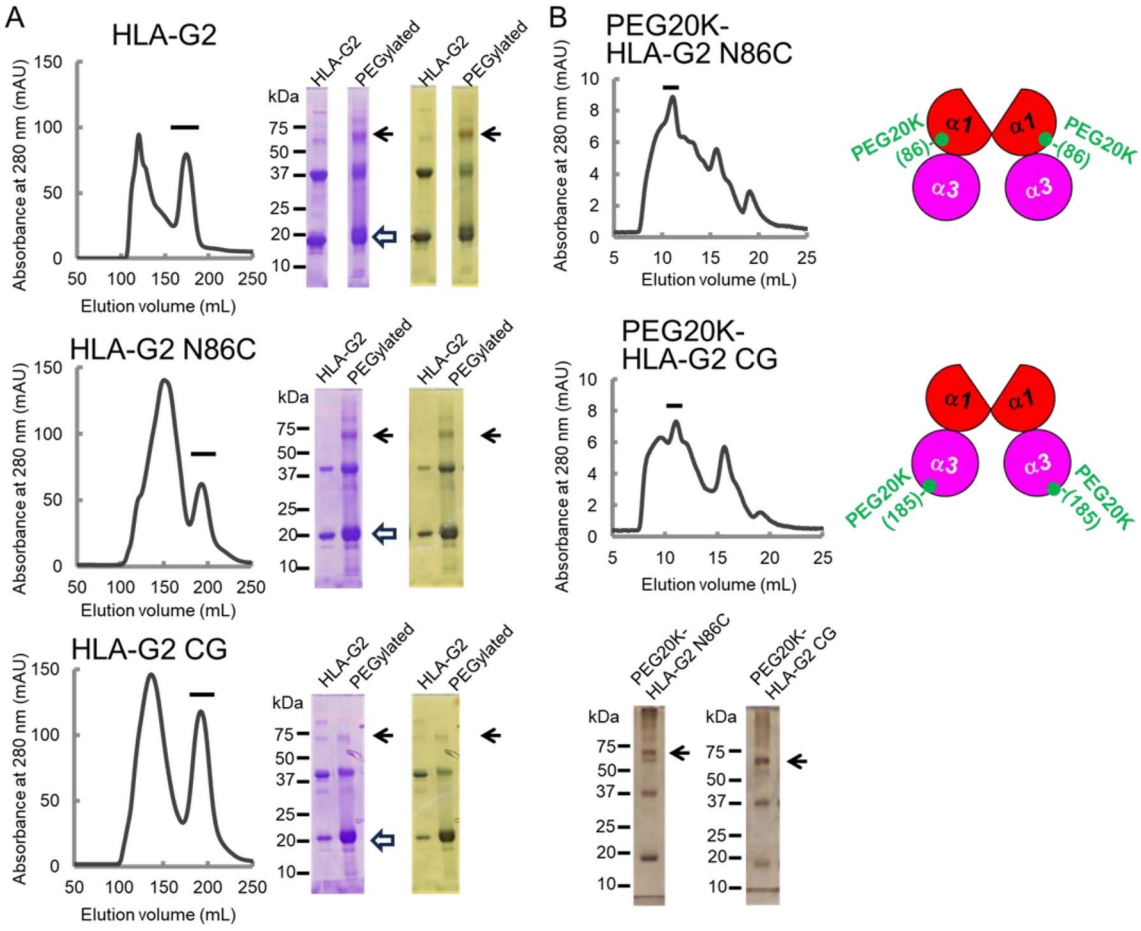

Fig. 4. PEGylation of soluble HLA-G2 homodimers at different positions by 20 kDa PEG. (**A**) Purification of soluble HLA-G2 homodimer proteins (left) and SDS-PAGE analysis of the peak fraction indicated by a black bar in each chromatogram (HLA-G2) and soluble HLA-G2 homodimers after the PEGylation reaction (PEGylated) under nonreducing conditions followed by CBB and BaI_2 staining. The black arrows indicate the PEGylated soluble HLA-G2 homodimer. The non-PEGylated soluble HLA-G2 homodimer (21 kDa via SDS-PAGE) is indicated by a white arrow. Multimerization of the non-PEGylated HLA-G2 resulted in the existence of a 42 kDa band in the gel due to disulfide bonds via Cys42. (**B**) Purification of the PEGylated soluble HLA-G2 homodimer mutants with 20 kDa PEG (upper) and SDS-PAGE analysis under nonreducing conditions followed by BaI_2 staining of the fractions shown by black bars in each chromatogram (lower). The black arrows indicate PEGylated HLA-G2, and non-PEGylated HLA-G2 (21 kDa) and multimerized HLA-G2-derived 42 kDa bands were observed. A schematic diagram of the domain structure of each soluble HLA-G2 homodimer is shown. Representative data from three independent experiments are shown. See Supplementary Fig. 4 for the uncropped gel images.

A

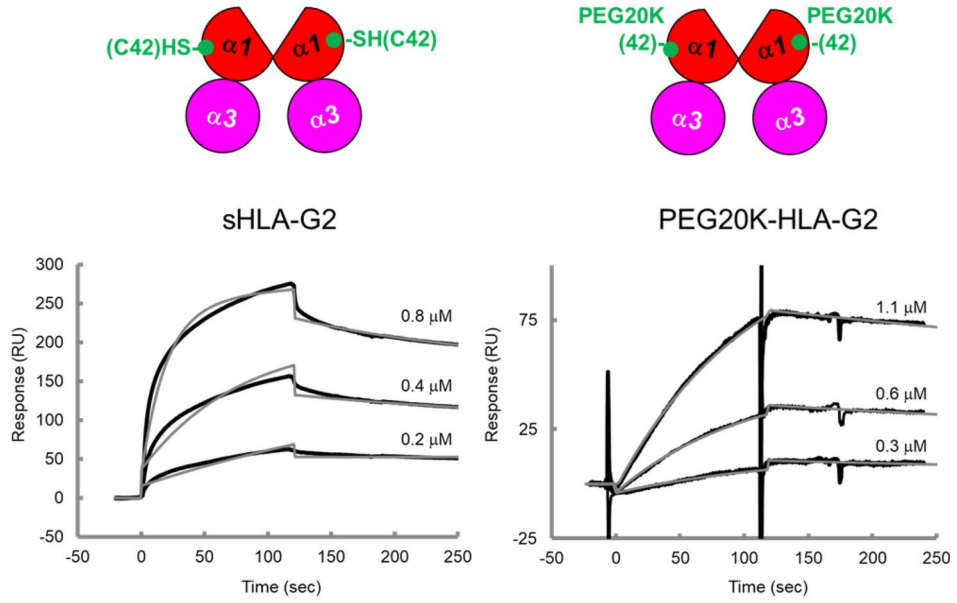

B

	k_{on} (1/Ms) ± SD	k_{off} (1/s) ± SD	K_D (M) ± SD
sHLA-G2	$6.4 \times 10^4 \pm 5.0 \times 10^4$	$8.6 \times 10^{-4} \pm 5.9 \times 10^{-4}$	$4.1 \times 10^{-8} \pm 7.4 \times 10^{-8}$
PEG20K-HLA-G2	$9.7 \times 10^3 \pm 7.3 \times 10^3$	$9.3 \times 10^{-4} \pm 3.0 \times 10^{-4}$	$13.8 \times 10^{-8} \pm 8.5 \times 10^{-8}$

Fig. 5. SPR analysis of the ability of sHLA-G2 and PEG20K-HLA-G2 to immobilize LILRB2 on the sensor chip. (**A**) Kinetic analysis of sHLA-G2 (left) and PEG20K-HLA-G2 (right) at the indicated concentrations. The binding response curves at each concentration of sHLA-G2 or PEG20K-HLA-G2 are shown by subtracting the response measured in the control flow cell (BSA) from the response in the sample flow cells (LILRB2). The response curves (black lines) were fitted locally with the Langmuir binding mode (gray lines), and apparent K_D values were calculated. LILRB2 was immobilized at approximately 500 RU for sHLA-G2 and approximately 270 RU for PEG20K-HLA-G2. BSA was immobilized at the same level for each experiment. This experiment was independently performed twice. (**B**) Kinetic parameters of the binding between sHLA-G2 or PEG20K-HLA-G2 and immobilized LILRB2 calculated by local fitting. The mean value and standard deviation (SD) were determined via six fitting data points (three concentrations in two independent experiments).

skin of both ears was significantly ameliorated by treatment with both HLA-G2 (vs. the PBS group) (Fig. 7D). Furthermore, compared with sHLA-G2, PEG20K-HLA-G2 significantly suppressed skin lesions.

Discussion

The soluble HLA-G2 homodimer is an immunosuppressive protein that can relieve clinical symptoms in a mouse model of clinically heterogeneous rheumatoid arthritis and systemic lupus erythematosus[10,11]. However, its free cysteine residue (Cys42) (Supplementary Fig. S1) may facilitate the formation of dimers and further aggregates of homodimers, which can be a problem for clinical use. Furthermore, the lack of glycosylation at Asn86 of the refolded soluble HLA-G2 homodimer might affect its stability. To overcome this, we established the optimal PEGylation method for HLA-G2. Compared with HLA-G2, PEG20K-HLA-G2 exhibited greater homogeneity, greater stability in vitro, and more substantial immunosuppressive effects in vivo. PEGylation is one of the established methods used to improve the pharmacokinetic properties of drugs. However, the high molecular weight of PEG might cause steric hindrance of the critical sites on a target protein, disturbing protein–protein interactions and resulting in the loss of their functions. Indeed, random PEG-HLA-G2 lost the ability to bind to its mouse receptor (Fig. 1). The complex structures of HLA-G2 with its receptors have not yet been clarified, but the binding region between HLA-G2 and human LILRB2 and its mouse orthologue PIR-B might be conserved. Based on the structures of the HLA-G1/LILRB1 and HLA-G1/LILRB2 complexes[14,15], LILRB2 binding is expected to be distributed in the α3 domain of soluble HLA-G2 homodimer. Therefore, PEG attachment at the lysine residues within the α3 domain (K94, K151, and K183) (Fig. 1B) might contribute to receptor binding. Additionally, PEG attachment at Cys42 can inhibit intramolecular disulfide bond formation and maintain molecular homogeneity (Fig. 6A,C). Furthermore, PEG20K-HLA-G2 showed a comparable LILRB2 binding affinity with soluble HLA-G2 homodimers (Fig. 5). The design of PEGylation can depend on the functional properties and biophysical characteristics of the target protein. Thus, the PEGylation and purification methods should be carefully investigated for each target protein.

PEG20K-HLA-G2 exhibited slightly increased stability against physical stresses in vitro (Fig. 6) and significantly suppressed clinical symptoms in atopic model mice (Fig. 7). Because both soluble HLA-G1 dimers/monomers and HLA-G2 homodimers may transmit inhibitory signals via PIR-B in mice, soluble HLA-G2 homodimer proteins might inhibit T-helper (Th)2 and Th17 cytokines and decrease the total IgE level, as shown in HLA-G1-administered mice[8]. Importantly, the receptor distributions of HLA-G1 and HLA-G2 differ between mice and humans. HLA-G1 binds to LILRB1 expressed in many immune cells (APCs, T cells, and NK cells) and to LILRB2 expressed in myeloid APCs, but HLA-G2 specifically binds to LILRB2 with higher affinity than does HLA-G1[3]. Because the distribution of PIR-B (myeloid APCs and B cells) is similar to that of LILRB2, targeting the LILRB2-HLA-G2 interaction is expected to be a target for specific and effective immunosuppression. Similarly, soluble β2m-free HLA-G1 homodimers (Supplementary Fig. S1) detected in human placental villous cytotrophoblast cells and spondylarthritis-related β2m-free HLA-B27 homodimers specifically bind to LILRB2[14,16,17]. These findings suggest that not only soluble HLA-G2 homodimers but β2m-free HLA class I heavy chain homodimers play significant roles and can have immunomodulation roles in vivo. Further in vivo and in vitro cellular analyses using human immune cells will be needed to understand the signals induced by soluble HLA-G2 homodimers or β2m-free HLA class I heavy chain homodimers in the future.

Recently, adverse drug effects due to anti-PEG antibody production have become a concern[18]. The soluble HLA-G2 homodimer induces immunosuppressive activity in CIA mice for more than a month after a single subcutaneous injection, possibly via immunosuppressive signaling at the antigen-presenting stage[10]. Although the detailed mechanism is unknown, long-term effects may reduce the administration frequency and are expected to reduce the risk of antigenicity as a PEG product. Furthermore, the combination of these drugs with other drugs is expected to further reduce their antigenicity and increase their efficacy.

This study examined the PEGylation conditions of immunosuppressive soluble HLA-G2 homodimers. Site-specific PEGylation at Cys42 via PEG20K (PEG20K-HLA-G2) resulted in increased stability against physical stresses in vitro. The immunosuppressive effects in vivo were significantly enhanced by PEGylation without immunogenicity. These observations suggest that HLA-G2 signaling via PIR-B in mice and LILRB2 in humans effectively regulate the immune system and induce anti-inflammatory effects. Further physiological expression and functional analyses of soluble HLA-G2 homodimers and the effects of their administration, such as tumorigenesis and viral infections, will be necessary in the future.

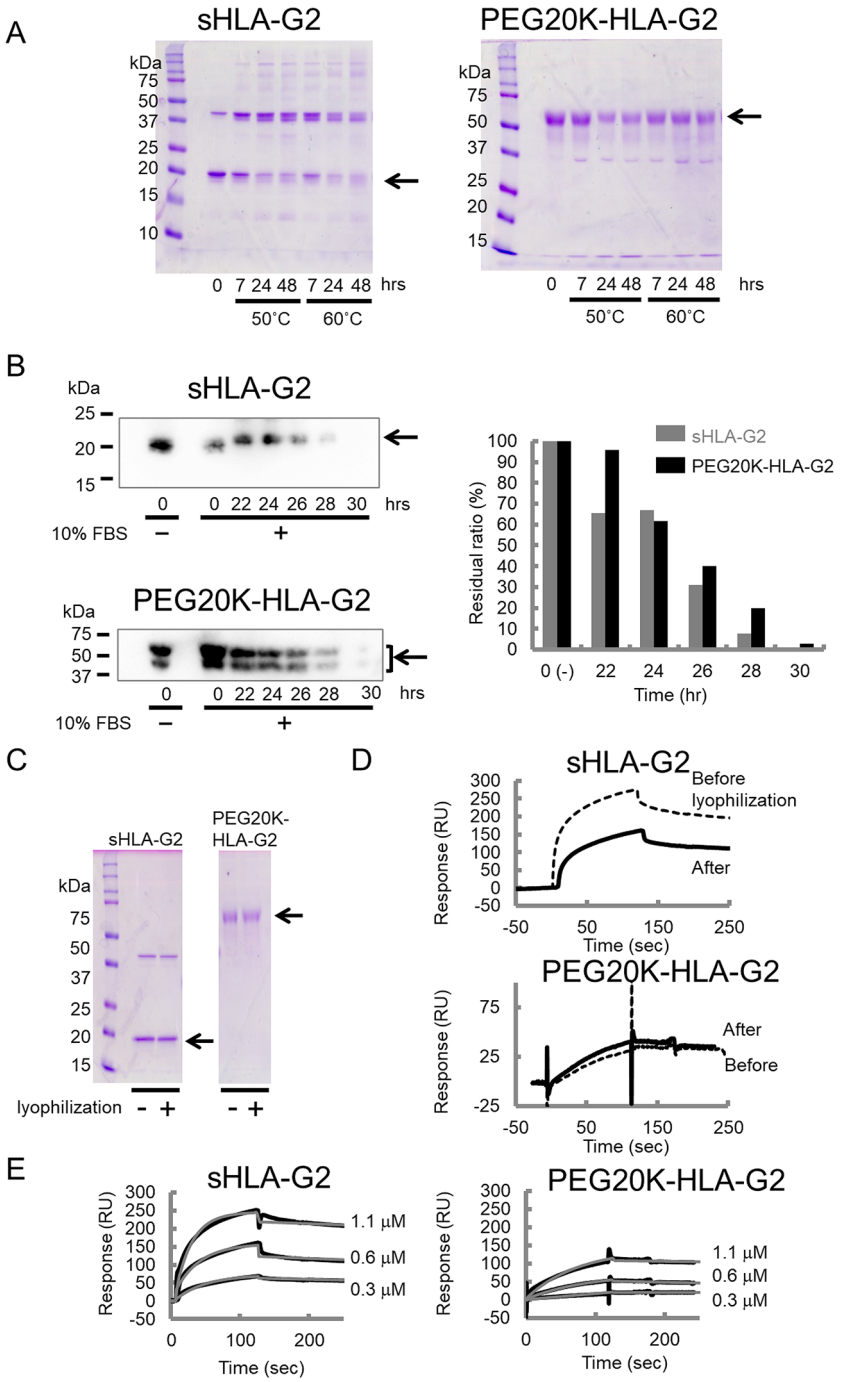

lyophylized	k_{on} (1/Ms) ± SD	k_{off} (1/s) ± SD	K_D (M) ± SD
sHLA-G2	$1.2 \times 10^4 \pm 6.7 \times 10^3$	$6.9 \times 10^{-4} \pm 2.3 \times 10^{-4}$	$6.4 \times 10^{-8} \pm 2.1 \times 10^{-8}$
PEG20K-HLA-G2	$1.1 \times 10^4 \pm 4.4 \times 10^3$	$1.2 \times 10^{-3} \pm 6.9 \times 10^{-4}$	$12.7 \times 10^{-8} \pm 6.4 \times 10^{-8}$

◀**Fig. 6**. In vitro stability analyses of sHLA-G2 and PEG20K-HLA-G2. (**A**) Heat stability was analyzed by SDS–PAGE under nonreducing conditions. The black arrow shows the band derived from each soluble HLA-G2 homodimer protein in the gel. The soluble HLA-G2 homodimer was partially multimerized during incubation as a disulfide-bonded 42 kDa band. Representative data from four independent experiments are shown. (**B**) Serum stability was analyzed by western blotting using MEM-G1 (the first antibody) and anti-mouse IgG-HRP (the second antibody). Left top: The intensity of the sHLA-G2 band after zero-hour incubation with FBS/without FBS was defined as 100%. Left bottom: Two bands of PEG20K-HLA-G2 were used for the quantification analysis, as PEG20K-HLA-G2 without serum was detected as two bands in this WB analysis. Right: The graph shows the residual ratio of sHLA-G2 (gray) and PEG20K-HLA-G2 (black) proteins in the WB. Representative data from four independent experiments are shown. (**C**) Lyophilization stability was analyzed by SDS–PAGE to compare degradation and aggregation under nonreducing conditions, followed by CBB staining. Representative data from two independent experiments are shown. (**D**) LILRB2 binding activity of sHLA-G2 and PEG20K-HLA-G2 (0.6 μM) before (dotted line) and after lyophilization (solid line) to the immobilized LILRB2. The sensorgrams were obtained by subtracting the responses measured in the BSA-immobilized flow cell (control) from those measured in the LILRB2-immobilized flow cell. (**E**) Kinetic analysis of lyophilized sHLA-G2 (left) and PEG20K-HLA-G2 (right) to immobilize LILRB2. The concentrations of the injected samples are shown on the right of the sensorgrams. This experiment was independently performed twice. The mean value and standard deviation (SD) were determined via six fitting data points (three concentrations in two independent experiments). See Supplementary Fig. 5 for the uncropped gel images of A and C, and Supplementary Fig. 6 for the full blot images and another result of B.

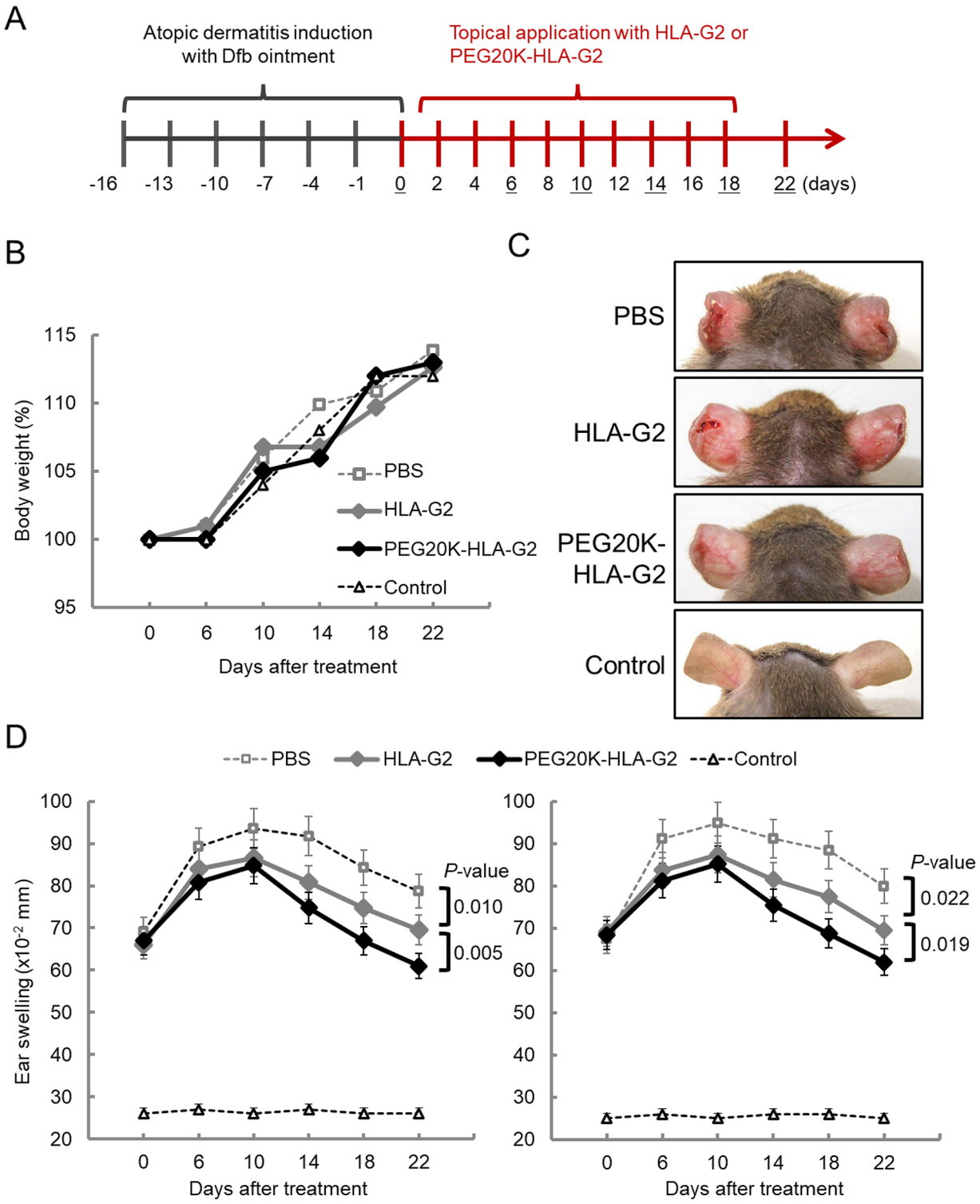

Fig. 7. Effect of PEG20K-HLA-G2 on Dfb ointment-induced atopic dermatitis in NC/Nga mice. NC/Nga mice without dermatitis induced by Dfb ointment were used as the control group. (**A**) Timeline of the experiments. Atopic dermatitis was induced with Dfb ointment treatment 6 times. The mice were treated with 5 μg of soluble HLA-G1 monomer, sHLA-G2, PEG20K-HLA-G2 or PBS every other day, and the thickness of the ear was monitored every 4 days, as indicated by underlines. (**B**) The average body weight changes in NC/Nga mice treated with soluble HLA-G2 homodimer proteins or PBS were monitored twice a week. (**C**) Macroscopic features of atopic dermatitis-like skin lesions in NC/Nga mice on Day 18. Representative data from four mice/group are shown. (**D**) Thickness of the left (left) and right (right) ears. The means ± standard error of the means (SEMs) (n = 4) and statistically significant differences are shown as *P* values (**P* < 0.05, ***P* < 0.01, ****P* < 0.001).

Data availability
The datasets generated and analyzed during the current study are available in this manuscript.

Received: 8 May 2024; Accepted: 31 December 2024
Published online: 20 January 2025

References
1. Kamishikiryo, J. & Maenaka, K. HLA-G molecule. *Curr. Pharm. Des.* **15**, 3318–3324. https://doi.org/10.2174/138161209789105153 (2009).
2. Kuroki, K. & Maenaka, K. Immune modulation of HLA-G dimer in maternal-fetal interface. *Eur. J. Immunol.* **37**, 1727–1729. https://doi.org/10.1002/eji.200737515 (2007).
3. Kuroki, K. et al. Cutting edge: Class II-like structural features and strong receptor binding of the nonclassical HLA-G2 isoform homodimer. *J. Immunol.* **198**, 3399–3403. https://doi.org/10.4049/jimmunol.1601296 (2017).
4. Bahri, R. et al. Soluble HLA-G inhibits cell cycle progression in human alloreactive T lymphocytes. *J. Immunol.* **176**, 1331–1339. https://doi.org/10.4049/jimmunol.176.3.1331 (2006).
5. Gonen-Gross, T. et al. Complexes of HLA-G protein on the cell surface are important for leukocyte Ig-like receptor-1 function. *J. Immunol.* **171**, 1343–1351. https://doi.org/10.4049/jimmunol.171.3.1343 (2003).
6. Naji, A. et al. Binding of HLA-G to ITIM-bearing Ig-like transcript 2 receptor suppresses B cell responses. *J. Immunol.* **192**, 1536–1546. https://doi.org/10.4049/jimmunol.1300438 (2014).
7. Kuroki, K. et al. The long-term immunosuppressive effects of disulfide-linked HLA-G dimer in mice with collagen-induced arthritis. *Hum. Immunol.* **74**, 433–438. https://doi.org/10.1016/j.humimm.2012.11.060 (2013).
8. Maeda, N., Yamada, C., Takahashi, A., Kuroki, K. & Maenaka, K. Therapeutic application of human leukocyte antigen-G1 improves atopic dermatitis-like skin lesions in mice. *Int. Immunopharmacol.* **50**, 202–207. https://doi.org/10.1016/j.intimp.2017.06.026 (2017).
9. Shiroishi, M. et al. Efficient leukocyte Ig-like receptor signaling and crystal structure of disulfide-linked HLA-G dimer. *J. Biol. Chem.* **281**, 10439–10447. https://doi.org/10.1074/jbc.M512305200 (2006).
10. Takahashi, A. et al. The immunosuppressive effect of domain-deleted dimer of HLA-G2 isoform in collagen-induced arthritis mice. *Hum. Immunol.* **77**, 754–759. https://doi.org/10.1016/j.humimm.2016.01.010 (2016).
11. Watanabe, H. et al. Therapeutic effects of soluble human leukocyte antigen G2 isoform in lupus-prone MRL/lpr mice. *Hum. Immunol.* **81**, 186–190. https://doi.org/10.1016/j.humimm.2019.11.002 (2020).
12. Furukawa, A. et al. Evaluation of the reactivity and receptor competition of HLA-G isoforms toward available antibodies: implications of structural characteristics of HLA-G isoforms. *Int. J. Mol. Sci.* https://doi.org/10.3390/ijms20235947 (2019).
13. Kanda, Y. Investigation of the freely available easy-to-use software "EZR" for medical statistics. *Bone Marrow Transplant* **48**, 452–458. https://doi.org/10.1038/bmt.2012.244 (2013).
14. Kuroki, K. et al. Structural and functional basis for LILRB immune checkpoint receptor recognition of HLA-G isoforms. *J. Immunol.* **203**, 3386–3394. https://doi.org/10.4049/jimmunol.1900562 (2019).
15. Shiroishi, M. et al. Structural basis for recognition of the nonclassical MHC molecule HLA-G by the leukocyte Ig-like receptor B2 (LILRB2/LIR2/ILT4/CD85d). *Proc. Natl. Acad. Sci. USA* **103**, 16412–16417. https://doi.org/10.1073/pnas.0605228103 (2006).
16. Giles, J. et al. HLA-B27 homodimers and free H chains are stronger ligands for leukocyte Ig-like receptor B2 than classical HLA class I. *J. Immunol.* **188**, 6184–6193. https://doi.org/10.4049/jimmunol.1102711 (2012).
17. Morales, P. J., Pace, J. L., Platt, J. S., Langat, D. K. & Hunt, J. S. Synthesis of beta(2)-microglobulin-free, disulphide-linked HLA-G5 homodimers in human placental villous cytotrophoblast cells. *Immunology* **122**, 179–188. https://doi.org/10.1111/j.1365-2567.2007.02623.x (2007).
18. Kozma, G. T., Shimizu, T., Ishida, T. & Szebeni, J. Anti-PEG antibodies: Properties, formation, testing and role in adverse immune reactions to PEGylated nano-biopharmaceuticals. *Adv. Drug. Deliv. Rev.* **154–155**, 163–175. https://doi.org/10.1016/j.addr.2020.07.024 (2020).

Acknowledgements
We thank Takashi Saito for technical support and Akira Matsuda for helpful discussions.

Author contributions
C.Y, K.K., N.M, H.W., A.T., and K.M. designed the experiments, performed research, and analyzed the data. C.Y., K.K., and K.M. wrote the paper.

Funding
This study was partly funded by the Japan Society for the Promotion of Science (JSPS) KAKENHI Grants JP23770102, JP25870019, JP18K06073, JP22H02749 (to K.K.), JP16J05871 (to A.T.) and JP20H05873 (to K.M.), and by the Japan Agency for Medical Research and Development (AMED) under Grant Numbers JP22ama121037, JP223fa627005, JP22gm1810004 (to K.M.), Hokkaido University, Global Facility Center, Pharma Science Open Unit, funded by the Ministry of Education, Culture, Sports, Science and Technology Grant "Support Program for Implementation of New Equipment Sharing System" (to K.M.), Hokkaido University Biosurface Project (to K.M.), the Naito Science & Engineering Foundation (to K.K.) and the Takeda Science Foundation (to K.M.).

Declarations

Competing interests
The authors declare no competing interests.

Consent for publication
All the authors read and approved the final manuscript.

Additional information

Supplementary Information The online version contains supplementary material available at https://doi.org/10.1038/s41598-024-85072-x.

Correspondence and requests for materials should be addressed to K.K. or K.M.

Reprints and permissions information is available at www.nature.com/reprints.

Publisher's note Springer Nature remains neutral with regard to jurisdictional claims in published maps and institutional affiliations.